

Atomic force microscopy on polymers and polymer related compounds

2. Monocrystals of normal and cyclic alkanes $C_{33}H_{68}$, $C_{36}H_{74}$, $(CH_2)_{48}$, $(CH_2)_{72}$ *

W. Stocker^{1,2}, G. Bar¹, M. Kunz², M. Möller³, S. N. Magonov^{1,**}, and H.-J. Cantow^{1,***}

¹Freiburger Material-Forschungszentrum FMF and ²Institut für Makromolekulare Chemie, Universität, Stefan-Meier-Strasse 31, W-7800 Freiburg, Federal Republic of Germany

³Department of Chemical Technology of the University of Twente, NL-7500 Enschede, The Netherlands

ABSTRACT

Atomic Force Microscopy (AFM) images have been recorded from the surfaces of platelet type monocrystals of linear alkanes, n-tritriacontane, $C_{33}H_{68}$, and n-hexatriacontane, $C_{36}H_{74}$. Structural details have been revealed in the range from several hundreds of nanometers down to the atomic scale. High resolution AFM micrographs of the linear alkanes show a regular pattern of elevations characterized by two main periodicities: $a_{AFM} = .70 \pm .02$ nm, $b_{AFM} = .52 \pm .05$ nm, $\gamma_{AFM} = 88 \pm 3^\circ$, and $a_{AFM} = .79 \pm .05$ nm, $b_{AFM} = .61 \pm .05$ nm, $\gamma_{AFM} = 87 \pm 3^\circ$, for $C_{33}H_{68}$ and $C_{36}H_{74}$, respectively. This structure is in fair agreement with the orthorhombic subcell of the bulk structure as confirmed by electron diffraction. Further, AFM results are in accordance with an orthorhombic unit cell for $C_{33}H_{68}$, and a monoclinic one for $C_{36}H_{74}$ under investigation. Consequently, the elevations in the AFM images can be assigned to individual methyl groups, which form the surface layer of a paraffine crystal.

A regular surface structure has also been observed in AFM images of platelet crystals of cyclic alkanes, cyclooctatetracontane $(CH_2)_{48}$, and cyclodoheptacontane $(CH_2)_{72}$. In these cases, the periodicities are characterized by $a_{AFM} = 1.10 \pm .01$ nm, $b_{AFM} = .85 \pm .01$ nm, $\gamma_{AFM} = 89 \pm 1^\circ$, and $a_{AFM} = 1.11 \pm .06$ nm, $b_{AFM} = .91 \pm .05$ nm, and $\gamma_{AFM} = 90 \pm 3^\circ$, for $(CH_2)_{48}$ and $(CH_2)_{72}$, respectively. The images are consistent with the arrangement of the adjacent reentry folds obtained from crystallographic data.

INTRODUCTION

Scanning probe techniques, i. e. scanning tunneling microscopy, STM [1], and atomic force microscopy, AFM [2], are novel tools for the analysis of surface structures, showing details with atomic resolution. While STM has been developed first and is widely used for conductive and semiconductive materials [3], AFM studies with a sub-nanometer resolution have been reported only recently. STM studies on monocrystals of organic conductors and superconductors show good agreement between STM pictures and the surface structure as derived from crystallographic data [4-6], and no evidence for surface reconstruction has been detected. This was also demonstrated for AFM by recent cooperative STM/AFM studies of the same monocrystals [7]. AFM images with atomic resolution were generally consistent with the corresponding STM data. Unlike other probe techniques, AFM does not require special interactions between the probe and the analyzed surface such as a tunneling current, magnetic force, etc. As based on probing interatomic van der Waals forces, AFM shows great promise to become a valuable tool for direct examination of surfaces of all kinds of materials. Thus, also AFM studies of nonconducting macromolecular materials can give detailed and important information on molecular surface structures. This has been demonstrated recently by AFM studies on surfaces of cold-

*Herrn Prof. Dr. Harald Cherdron zu seinem 60. Geburtstag herzlich gewidmet

**Permanent address: Institute of Chemical Physics of the USSR Academy of Sciences, Kosygin ul. 4, SU-117977 Moscow, USSR

***To whom offprint requests should be sent

extruded polyethylene [8], epitaxially crystallized isotactic polypropylene [9], and of monocrystals of diacetylene and polydiacetylene derivatives [10]. This paper is directed towards the study of low molecular weight oligomer crystals with well established and regular lamellar surfaces consisting of chain ends and tight folds as model compounds to approach AFM research on the less defined polymeric homologues. Surfaces of monocrystals of linear and cyclic alkanes, n-tritriacontane, n-hexatriacontane, cyclooctatetracontane, and cyclodoheptacontane have been examined.

EXPERIMENTAL

AFM experiments were carried out with a Nanoscope II microscope (Digital Instruments, Inc., Santa Barbara, Cal., USA) at ambient conditions. Sample surfaces were scanned by a tiny pyramidal Si_3N_4 tip which is attached to a microfabricated cantilever (200 μm triangular base). Deflections of the cantilever were registered via deflection of a laser beam. The largest scan area was 700 x 700 nm (head type A). Cantilevers had a force constant of .06 and .12 N/m. Scanning line frequencies were 1Hz for large scale scans and up to 39 Hz for smaller areas. Thermal drift of images was observed even by scanning at highest frequencies. This resulted in minor neglectable deviations in the structure parameters, i. e. repeat distances and angles. In most experiments, images were taken repeatedly whereby samples were scanned in different directions. This provides an important opportunity to verify observed images.

An important requirement for samples to be studied by AFM is flatness of the surface. Monocrystals of linear and cyclic alkanes have a platelet shape, and large lamellar surfaces are suitable for AFM studies. Monocrystals of orthorhombic n-tritriacontane, $\text{C}_{33}\text{H}_{68}$, of monoclinic n-hexatriacontane, $\text{C}_{36}\text{H}_{74}$, of cyclooctatetracontane, $(\text{CH}_2)_{48}$, and of cyclodoheptacontane, $(\text{CH}_2)_{72}$, were prepared as described elsewhere [11-12]. Electron diffraction experiments on $\text{C}_{33}\text{H}_{68}$ and $\text{C}_{36}\text{H}_{74}$ monocrystals were done with a 100 kV Phillips 400 electron microscope. SCHAKAL, a molecular graphics computer software [13], was used for construction of the atomic picture of the surfaces based on X-ray analysis data of $\text{C}_{33}\text{H}_{68}$ [14] and $(\text{CH}_2)_{36}$ [15].

RESULTS AND DISCUSSION

n-Alkanes

AFM images of the surface of a platelet monocrystal of n-tritriacontane, $\text{C}_{33}\text{H}_{68}$, are presented in Figs. 1A-C. Fig. 1A shows an image obtained with large scan width (475 x 475 nm). Only relatively coarse details are resolved. Cuts of two crystals with well defined edges and flat surfaces are visible. When the scanning width is decreased, a regular pattern is revealed at higher magnification which corresponds to the packing of molecules in the crystal (see Fig. 1B). This is seen more clearly in Fig. 1C where roundly shaped elevations or 'hills' form a two-dimensional lattice. The two-dimensional Fourier-transform is characterizing the symmetry. Periodicities were determined in the directions indicated in Fig. 1B: $a_{\text{AFM}} = .70 \pm .02$ nm, $b_{\text{AFM}} = .52 \pm .05$ nm, and $\gamma_{\text{AFM}} = 88 \pm 3^\circ$. Arbitrary rotation of the scanning direction results in the corresponding reorientation of the AFM pattern without affecting the observed structure. Figs. 1B and 1C are consistent with the crystallographic [001] plane of the orthorhombic $\text{C}_{33}\text{H}_{68}$: $a_{\text{CR}} = .744$ nm, $b_{\text{CR}} = .496$ nm, and $\gamma = 90^\circ$ [14]. As the [001] plane corresponds also to the lamellar surface, which is formed by the methyl end groups of the n-alkane, Fig. 1C turns out to be a molecular visualization of the lamellar surface of the orthorhombic n-tritriacontane monocrystal. The selected area diffraction pattern of this monocrystal (SAED, Fig. 1D) confirms the orthorhombic symmetry of the surface of $\text{C}_{33}\text{H}_{68}$, where the chains are arranged perpendicular to this surface. Hills of AFM map re-

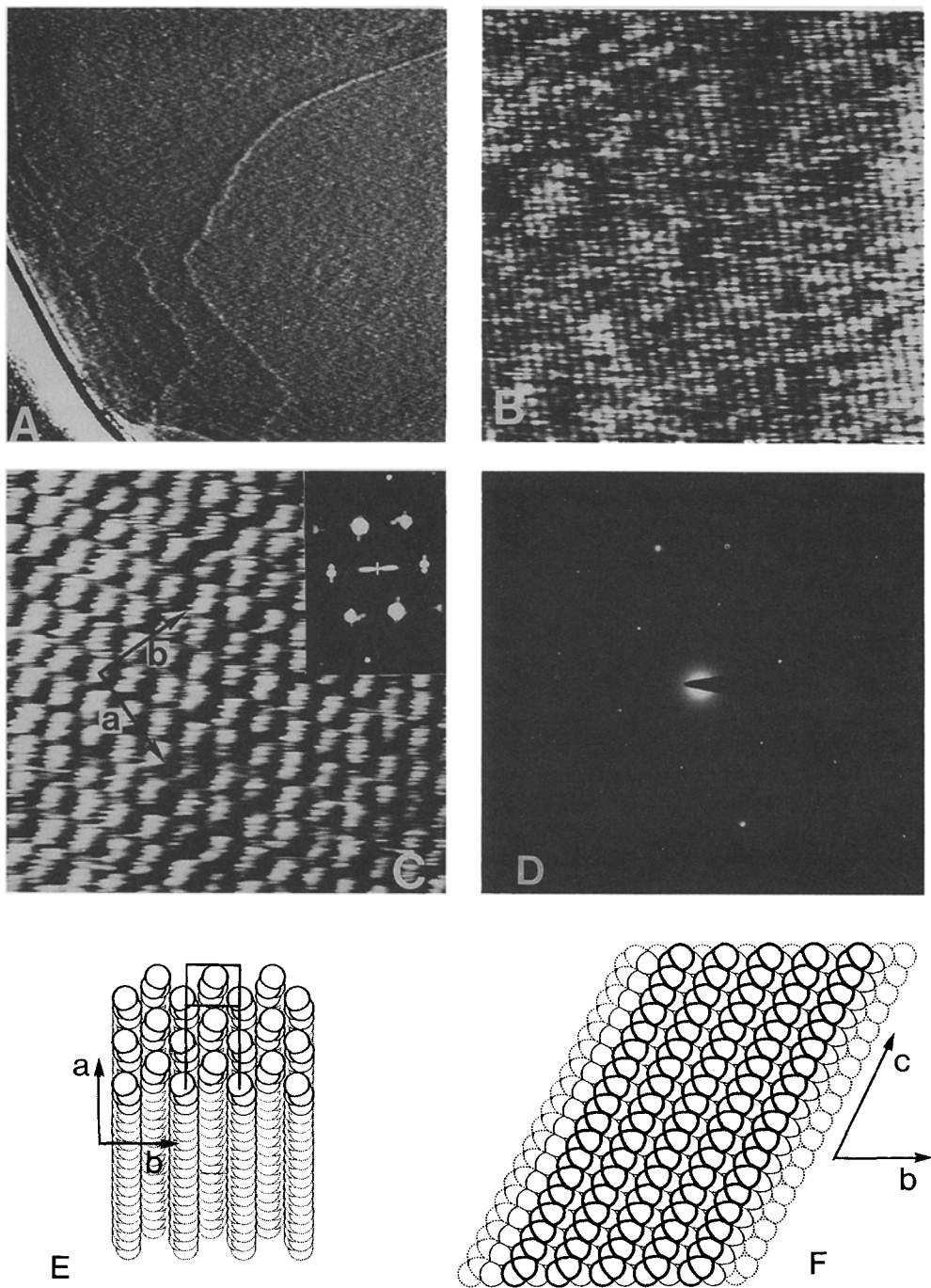


Figure 1: AFM images of orthorhombic n-tritriacontane **A** - Top-view, 475 x 475 nm
B - Top-view, 14,2 x 14,2 nm **C** - Top-view, 5,7 x 5,7 nm, with 2D-Fourier transform
D - Selected area electron diffraction pattern (SAED) of n-tritriacontane
E Crystal structure of monoclinic n-hexatriacontane **E** - [001] plane **F** - [100] plane

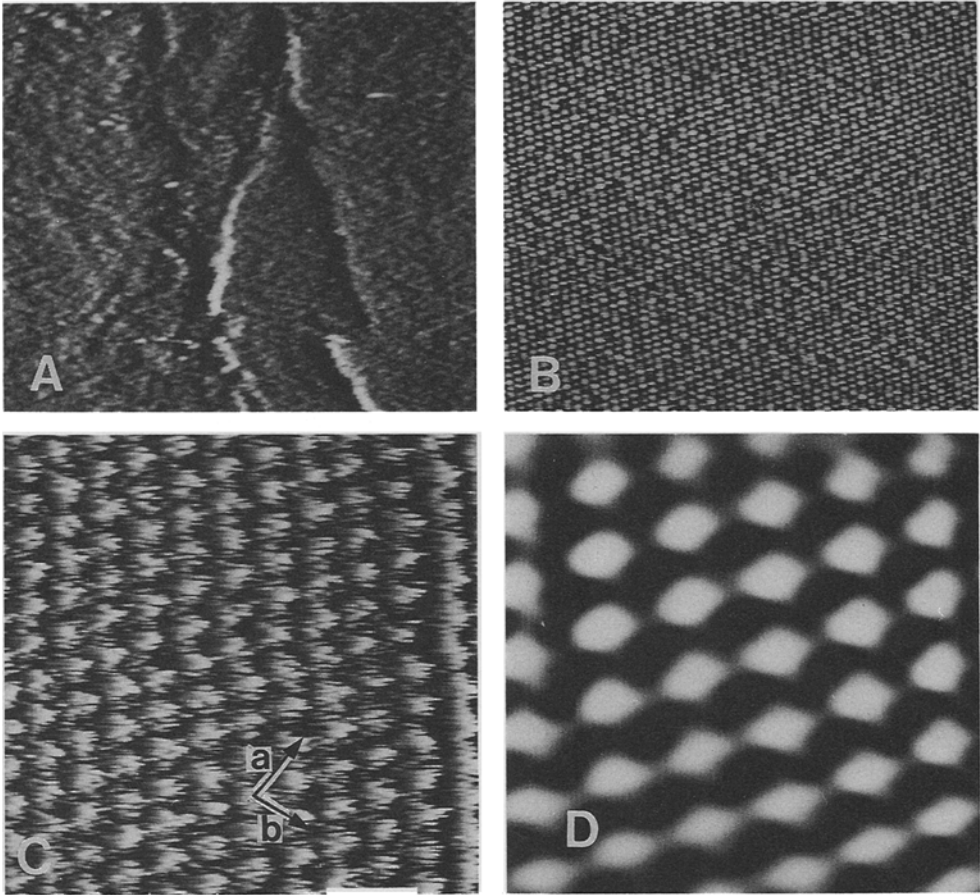
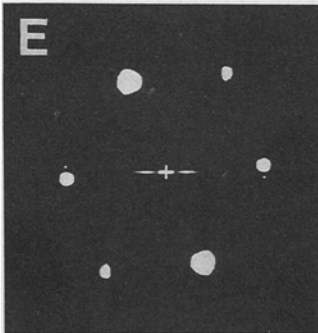
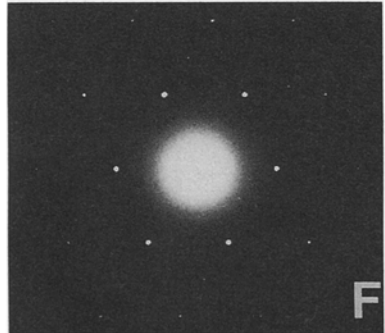


Figure 2: AFM top view images of n-hexatriacontane, $C_{36}H_{74}$
- **A** - 570 x 500 nm - **B** - 28.5 x 24.9 nm - **C** - 5.7 x 5.56 nm - **D** - 2.85 x 2.78 nm



At left: **E** - 2D-Fourier transform of 2C
At right: **E** - (SAED) of n-hexatriacontane



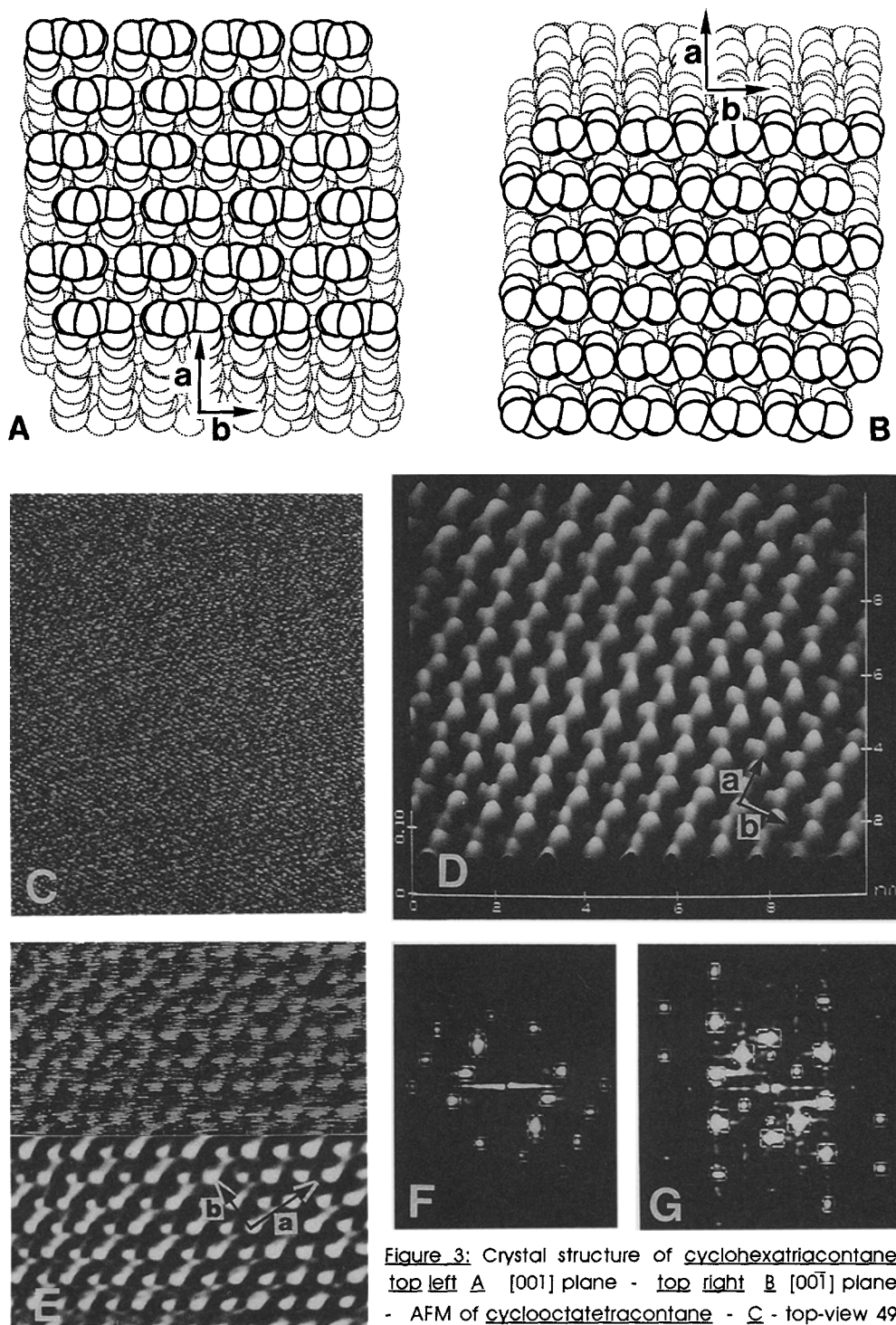


Figure 3: Crystal structure of cyclohexatriacontane top left **A** [001] plane - top right **B** [001] plane - AFM of cyclooctatetracontane - **C** - top-view 49 x 57 nm **D** - 3D-view at 60° rotation - **E** - top-view 8.1 x 9.5 nm - at 30° rotation - part of image after filtration **E** - 2D FT of **D** **G** - 2D FT of **E**

present individual methyl groups whereby atomic details, i. e. hydrogen and carbon atoms, cannot be distinguished. A corresponding assignment was proposed for the AFM images of DL-leucine monocystals [16]. Also in this case, individual carbon and hydrogen atoms have not been resolved. However, at ambient temperature, fast rotation of the methyl group around the α -carbon-carbon bond is well established [11] and gives mandatory explanation for the diffusive pattern. Variations in the height have been estimated to be approximately .3 Å. An interpretation of the surface profile is not possible definitely at present due the missing theoretical understanding of AFM imaging.

Figs. 1E and F present the SCHAKAL-simulation of the monoclinic n-hexatriacontane, for the [001] and the [100] plane. The tilt angle of 19.1° is evident. AFM images of platelet crystal surfaces of $C_{36}H_{74}$ are shown in Figs. 2A - D. While the image in Fig. 2A, which was obtained at large scan width, does not show a well defined structure, images with a well resolved peculiar structure were obtained at smaller scan width (Figs. 2B, C, D). The pattern of elevations has been analyzed by means of a two-dimensional Fourier transformation shown in Fig. 2E. The main periodicities are almost orthogonal: $a_{AFM} = .79 \pm .05$ nm, $b_{AFM} = 0.61 \pm .05$ nm, and $\gamma_{AFM} = 87 \pm 3^\circ$. Electron diffraction experiments have been employed (Fig. 2F) to check that the packing of methylene segments is in accordance with an orthorhombic subcell with the repeat distances $a_{CR} = .742$ nm, $b_{CR} = .496$ nm [15]. The relatively close agreement with the AFM periodicities indicates that - like in the case of tritriacontane - the picture represents the arrangement of methyl groups at the surface of n-hexatriacontane lamellar crystals.

Two different crystal modifications have been reported for n-hexatriacontane, one with monoclinic unit cell [15] ($a_{CR} = .742$ nm, $b_{CR} = .557$ nm, $c_{CR} = 4.835$ nm) and the other with an orthorhombic unit cell ($a_{CR} = .742$ nm, $b_{CR} = .496$ nm, $c_{CR} = 9.514$ nm), $\beta = 119,1^\circ$ [17]. In both cases the methylene groups form an orthorhombic subcell ($a_{CR} = .742$ nm, $b_{CR} = .495$ nm, $c_{CR} = .255$ nm), and the two structures differ by the inclination of the all trans-planar zig-zag chains with respect to the lamellar surface. The AFM results - the top view image of the methyl groups and the two-dimensional FT - confirm the monoclinic modification for the studied n-hexatriacontane monocystals.

Cycloalkanes

Also monocystals of $(CH_2)_{236}$, $(CH_2)_{248}$, and $(CH_2)_{272}$ possess well defined flat surfaces and can be grown to relatively large size. They pack in a monoclinic crystal structure. The molecules crystallize in lamellae. Two parallel all trans-planar zig-zag methylene strands are connected at both sides by well defined gg₂g₂ folds. The lamellar surfaces are formed by the adjacent reentry folds. As the surface of a platelet monocystal is known to be formed by the outermost lamellar surface, AFM investigations allow to study the fold structure.

Table 1: AFM parameters of cyclooctatetradecane at different scanning angles, 3 series of experiments. Overall-average $a_{AFM} = 1.10_2$ nm, $b_{AFM} = .84_7$ nm, $\gamma_{AFM} = 88.9^\circ$

Rot/°	a_{AFM}	b_{AFM}	$\gamma_{AFM}/^\circ$
0	1.0 ₇	.86	89 ₀
30	1.0 ₉	.84	87 ₈
60	1.1 ₀	.82	87 ₄
90	1.1 ₂	.83	88 ₂
120	1.1 ₄	.83	89 ₀
150	1.0 ₉	.85	90 ₀
180	1.1 ₂	.86	89 ₀
1. exp	1.10 ₂	.84 ₁	88 ₇
2. exp	1.09 ₆	.83 ₉	88 ₅
3. exp	1.10 ₉	.86 ₀	89 ₆

Almost identical crystal conformations have been observed for cyclohexatriacontane and cyclodoheptacontane, basically varying in the length of the trans-planar strands. The crystallographic parameters for cyclooctatetracontane, $(\text{CH}_2)_{48}$ are $a_{\text{CR}} = 1.033$ nm, $b_{\text{CR}} = .819$ nm, $c_{\text{CR}} = 5.77$ nm, $\beta_{\text{CR}} = 109.7^\circ$, $\gamma_{\text{CR}} = 90^\circ$ [18]. Figs. 3C-E show a series of AFM images of $(\text{CH}_2)_{48}$. At the smaller magnification in Fig. 3C, the flat crystal surface does not show a particular fine structure. Smaller scale images of the lamellar surface were recorded varying the scanning direction towards the sample by 30° steps over 180° . This procedure allows to verify the observed structure but also to optimize the quality of the recorded images. We succeeded in obtaining high quality images at almost all orientation angles as shown at the examples of Figs. 3C, D and E. All pictures show the same well defined pattern of longish elevations with .3 to .4 nm in length. The repeat distances, a_{AFM} , b_{AFM} and γ_{AFM} were evaluated in the directions as indicated in Fig. 3D. Averaged values as obtained at different scanning angles are listed in Table 1. Comparison of the AFM and crystallographic parameters allows the conclusion that the examined surface corresponds to the $[001]$ or the $[00\bar{1}]$ plane. To allow a direct interpretation of the AFM image, topviews of the $[001]$ or the $[00\bar{1}]$ plane were reconstructed from crystallographic data by means of SCHAKAL program. Figs. 3AB demonstrate the arrangements of C atoms in the lamellar surface corresponding to the $[001]$ and the $[00\bar{1}]$ planes. In order to simplify the picture, H atoms are not shown. The stereoscopic pictures indicate the regular variations in xyz position of the surface atoms. Clearly the same zig-zag pattern is obvious along the a-direction which is distinctively seen in the AFM images. Thus, it appears reasonable to assign the examined surface to the $[001]$ plane, where the AFM hills represent the most elevated segment of a tight adjacent reentry fold. Individual atoms have not been resolved.

Similar like cyclooctatetracontane also cyclodoheptacontane crystallizes in lamellae whose surfaces are formed by defined ggtgg folds. AFM images of cyclodoheptacontane, which are presented in Figs. 4A and B, correspond to those of cyclooctatetracontane in Fig. 3 and show regular pattern of slightly elongated elevations. The image can be described by an almost orthogonal lattice with $a_{\text{AFM}} = 1.11 \pm 0.06$ nm, $b_{\text{AFM}} = .91 \pm 0.05$ nm, and $\gamma_{\text{AFM}} = 90 \pm 3^\circ$. Also to be expected, these parameters are close to the crystallographic interchain distances in the $[001]$ plane. As the consequence of the nearly orthogonal orientation of the c-axis, the lamellar surface corresponds to the crystallographic $[001]$ plane. The height profile in the AFM picture can be assigned to the most elevated $\text{CH}_2\text{-CH}_2$ -segments of the $-\text{CH}_2\text{-CH}_2\text{-CH}_2\text{-CH}_2$ -folds.

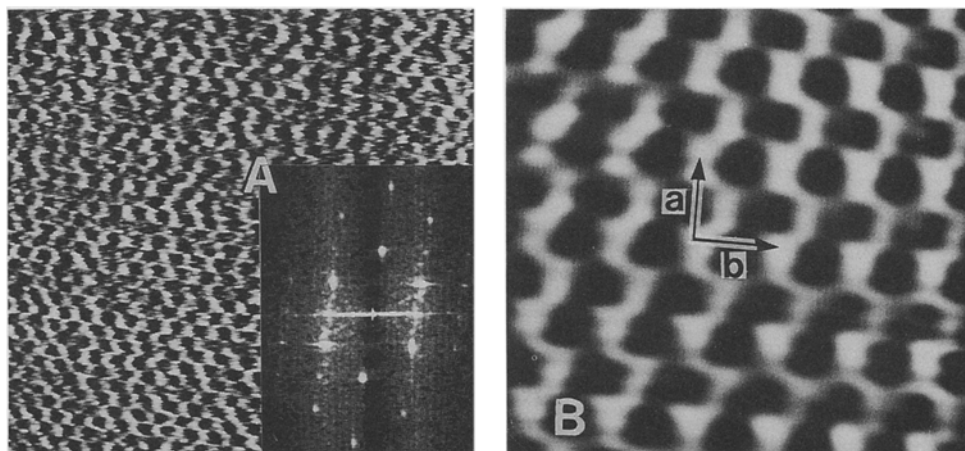


Figure 4: AFM of cyclodoheptacontane, $(\text{CH}_2)_{72}$ **A** - 19 x 19 nm and 2D FT **B** - 5.7 x 5.7 nm

CONCLUSIONS

The experimental results presented above demonstrate the potential of atomic force microscopy for quantitative surface structure analysis of organic monocrystals. For both types of alkanes - linear and cyclic - well resolved AFM images have been obtained and assigned. Even such structural details like differences in periodicities of orthorhombic and monoclinic n-alkanes and variations in molecular arrangement of the [001] and [001] planes of cyclic alkanes were detected.

The examined normal and cyclic paraffines can be regarded as well defined models for polyethylene, demonstrating the packing of strands and adjacent reentry of folded chains. Thus, AFM may become a powerful tool for the examination of important structural details of crystalline polymers, i.e. stems, folds, and end groups, and consequently also structural defects can be visualized by AFM.

ACKNOWLEDGEMENTS

We thank cordially to Dr. Egbert Keller for modifying the SCHAKAL program for the visualization of surfaces and to Dr. Markus Drechsler for measuring the SAED of $C_{33}H_{68}$. To Prof. Dr. Gerd Strobl we are grateful for the $C_{33}H_{68}$ sample and for helpful discussions. Cooperation with Dr. Vergil Elings from Digital Instruments is gratefully acknowledged. We are indebted to Eva Schill-Wendt for her photographic work.

REFERENCES

1. Binnig G, Rohrer H, Gerber Ch, Weibel E (1982) Phys Rev Lett 49:52
2. Binnig G, Quate C F, Gerber Ch (1986) Phys Rev Lett 56:930
3. 'Scanning Tunneling Microscopy and Related Methods' Böhm R, Garcia N, Rohrer H (eds) (1990) Kluwer Acad Publ Dordrecht
4. Magonov S N, Schuchhardt J, Kempf S, Keller E, Cantow H-J (1991) Synth Met 40:59
5. Magonov S N, Kempf S, Rotter H, Cantow H-J (1991) Synth Met 40:73
6. Magonov S N, Bar G, Keller E, Yagubskii E B, Cantow H-J (1991) Synth Met 40:247
7. Magonov S N, Bar G, Laukhina E E, Yagubskii E B, Cantow H-J (1991) in prep
8. Magonov S N, Qvarnström K, Elings V, Cantow H-J (1991) Polym Bull in press
9. Lotz B, Stocker W, Wittmann J C, Magonov S N, Cantow H-J (1991) Polym Bull in press
10. Magonov S N, Bar G, Cantow H-J, Bauer H-D, Müller I, Schwoerer M (1991) Polym Bull in press
11. Möller M, Cantow H-J, Drotloff H, Emeis D, Lee K-S, Wegner G (1987) Makromol Chem 187:1237
12. Schill G, Zürcher C, Fritz H (1978) Chem Ber 111:2901
13. Keller E J (1989) J Appl Crystallogr 22:19
14. Strobl G, Ewen B, Fischer E W, Piesczek (1974) J Chem Phys 61:5257
15. Shearer H M M, Vand V (1956) Acta Cryst 9:379
16. Gould S, Marti O, Drake B, Hellemans L, Bracker C E, Hansma P K, Keder N L, Eddy M M, Stucky G D (1988) Nature 332:332
17. Teare P W (1959) Acta Cryst 12:19
18. Trzebiatowski T, Dräger M, Strobl G R (1982) Macromol Chem 183:731